Laser and Particle Beams (2007), *25*, 523–540. Printed in the USA.

DOI: 10.1017/S026303460700064X

Numerical modeling of heavy ion induced stress waves in solid targets

N.A. TAHIR,[1] V. KIM,[2] A. MATVECHEV,[2] A. OSTRIK,[2] I.V. LOMONOSOV,[2] A.R. PIRIZ,[3] J.J. LOPEZ CELA,[3] AND D.H.H. HOFFMANN[4]

[1]Gesellschaft für Schwerionenforschung, Darmstadt, Germany
[2]Institute for Problems of Chemical Physics, Chernogolovka, Russia
[3]E.T.S.I. Industriales, Universidad de Castilla-La Mancha, Ciudad Real, Spain
[4]Institut für Kernphysik, Technische Universität Darmstadt, Germany and Gesellschaft für Schwerionenforschung, Darmstadt, Germany

(RECEIVED 25 June 2007; ACCEPTED 23 July 2007)

Abstract

This paper presents numerical simulations of thermodynamic and hydrodynamic response for solid targets that are irradiated with strongly bunched, highly focused, intense beams of energetic uranium ions. The main purpose of this work is to study the behavior of thermal stress waves induced in such targets by the incident ion beam. These theoretical studies will complement the experimental investigations that will be carried out in the near future at the Gesellschaft für Schwerionenforschung (GSI) plasma physics experimental area. These experiments will be performed using the existing heavy ion synchrotron, SIS18, which delivers 4×10^9 uranium ions in a single bunch with a length of about 125 ns. Other time structures, for example, a pulse that consists of a series of bunches, are also possible. The particle energy is on the order of 400 MeV/u and the beam can be focused to sub millimeter radius. This information concerning material response under intense beam loading will have important implications on designing a viable production target for the superconducting fragment separator, Super-FRS, which is going to be constructed at the future facility for antiproton and ion research (FAIR), Darmstadt, Germany, for the production and separation of exotic nuclei.

Keywords: Elastic plastic behavior; FAIR; Fragment separator; High energy density physics; Intense heavy ion beams; Radioactive beams

1. INTRODUCTION

The new very powerful facility for antiproton and ion research (FAIR) at Darmstadt (Henning, 2004); will include construction of two synchrotron rings (SIS100 and SIS300) that will substantially increase the existing accelerator capabilities of the Gesellschaft für Schwerionenforschung Darmstadt. The new facility will deliver high quality heavy ion beams including uranium with unprecedented intensities of about 10^{12} particles per spill. A wide range of particle energies (400 MeV/u–2.7 GeV/u) will be available while the beam focuses on a 1 mm spot. Both fast and slow extraction options will be available for the beam. In the former case, the bunch length will be on the order of 50–100 ns, while in the latter case, one will have a quasi-uniform beam power. Availability of such high intensity beams will enable scientists to perform experiments in different fields of research including High-Energy-Density (HED) physics (Tahir *et al.*, 2000*a*, 2000*b*, 2001*a*, 2001*b*, 2003, 2005*a*, 2005*b*, 2006, 2007*a*, 2007*b*; Piriz et *al.*, 2002, 2003, 2005, 2006, 2007*a*, 2007*b*, Temporal *et al.*, 2003, 2005; Lopez Cela *et al.*, 2006; Hoffmann *et al.*, 2005) and production of radioactive beams (Geissel *et al.*, 2003; Tahir *et al.*, 2003*b*, 2005*c*). Another huge accelerator facility that is being built in Europe is the large hadron collider (LHC) at CERN. Recently, theoretical studies were carried out to investigate some of the safety issues related to this impressive machine (Tahir *et al.*, 2005*d*). This work has shown that the LHC can also be used to study HED physics (Tahir *et al.*, 2005*e*).

The production target is a very important part of the fragment separator which should survive and remain intact during all experimental shots that are carried out over an extended period of time. Detailed theoretical investigations have shown (Tahir *et al.*, 2003*b*, 2005*c*) that the high instantaneous power deposition by fast extracted beams

Address correspondence and reprint requests to: N. A. Tahir, Gesellschaft für Schwerionenforschung Darmstadt, Planckstrasse 1, 64291 Darmstadt, Germany. E-mail: n.tahir@gsi.de

(up to $\sim$ 200 GW in case of full intensity of a high-Z beam) may lead to destruction of a solid target even by a single ion pulse. The specific power deposition must be reduced to avoid destruction of the target. One way to achieve this goal is by increasing the size of the beam spot. However, the resolving power of the fragment separator is inversely proportional to the dimensions of the focal spot in the horizontal direction (X-direction). Transmission of the radioactive nuclides through the fragment separator, on the other hand, depends only on the spot size in the Y-direction. It has therefore been found advantageous to use an elliptic focal spot, which will fulfill the necessary conditions for good resolution and reasonable transmission, and at the same time it will have large enough area to lead to an acceptable level of power deposition in many cases of interest. It is important to note that with the full intensity of the uranium beam, production target made of solid graphite will always be destroyed by a single pulse, if one uses a focal spot size to satisfy the above considerations. It has been proposed (Nolen *et al.*, 2003; Fabich *et al.*, 2003) to use a liquid metal jet target as an alternative. Detailed three-dimensional (3D) numerical simulations for interaction of a liquid lithium jet target with the full intensity of the uranium beam have recently been carried out and reported elsewhere (Tahir *et al.*, 2007*c*). These simulations have provided very useful information that will allow one to develop a viable liquid metal target for the Super-FRS.

In case of a solid target, there are two important parameters that determine if the target will survive during the experiment. First, the temperature should remain below the melting or sublimation temperature of the material. Second, the thermal stress induced by the beam should always be less than the tensile strength of the material, so that the stress waves do not inflict permanent damage to the material before they are damped out. Due to the technical challenges involved in construction and operation of a liquid metal jet target, it is desirable to use a rotating wheel type solid graphite target (Tahir *et al.*, 2005*c*; Heidenreich, 2002) as long as the above two critical parameters for graphite are not exceeded. Sophisticated theoretical calculations have shown (Tahir *et al.*, 2007*c*) that one may be able to use a solid graphite target for a beam of up to 10^{11} uranium ions per bunch. However, experimental data on the response of solid graphite material under intense beam loading is also essential in order to construct a viable target for the Super-FRS. For this purpose, experiments have been planned at the GSI Plasma Physics experimental area to study some of the material properties of graphite using the uranium beam that is available at the existing heavy ion synchrotron, SIS18. Since the material properties including elastic-plastic behavior of matter under dynamic conditions is of considerable scientific and technological interest, targets made of other materials, for example, W, Cu, Ta, and Pb will also be studied. We have done numerical simulations on beam-target heating using the beam and target parameters that will be used in the experiments. We believe that this data will be helpful in understanding and interpreting the experimental results.

In Section 2, we describe the problem while the beam and target parameters are noted in Section 3. Capabilities of the 3D computer code used to do these simulations are discussed in Section 4. Numerical simulation results are reported in Section 5 while conclusions drawn from this work are noted in Section 6.

2. PROBLEM DEFINITION

It is to be noted that the transverse power profile in the focal spot is considered to be Gaussian. Previous calculations have shown (Tahir *et al.*, 2005*c*) that for 10^{10} uranium ions per bunch, the temperature and the pressure in the graphite target are below their respective critical values if one uses a focal spot with $\sigma_x = 1.0$ mm and $\sigma_y = 6.0$ mm. The corresponding specific energy deposition is 0.08 kJ/g. In case of 10^{11} uranium ions per bunch, the target would survive if one assumes $\sigma_x = 2.0$ mm and $\sigma_y = 12.0$ mm which are the limiting values allowed by isotope resolution and transmission considerations. The specific energy deposition in this case comes out to be 0.1 kJ/g. These conditions can be generated using the available uranium beam at the SIS18 that has a lower intensity, provided it is focused to a smaller spot size. This technique will be used in the forthcoming experiments that will be performed at GSI. In general, the material properties like yield strength and shear modulus have been measured only at room temperature, and very little is known about material behavior under dynamic conditions. It has therefore been planned to use numerous targets of other materials including W, Cu, Ta, and Pb in addition to graphite. Such studies will be a very valuable contribution to this field.

3. BEAM AND TARGET PARAMETERS

In this section, we give beam and target parameters for those experiments that will be performed to study the elastic limit, plastic behavior, and material rupture under beam loading.

3.1. Copper Target

The target is cylinder with a length equal to 7 mm and radius equal to 5 mm. One face of the cylinder is irradiated with a uranium beam having particle energy of 400 MeV/u. The beam pulse consists of two bunches, each having a FWHM of 80 ns, and the total pulse duration is 500 ns. The beam focal spot size (FWHM of the Gaussian power distribution in transverse direction) is assumed to be 0.5 mm. Two different values for beam intensity, N are used.

3.1.1. Case I

$N = 5.0 \times 10^7$ ions per pulse is considered to study the elastic properties of Cu.

3.1.2. Case II

$N = 1.5 \times 10^8$ ions per pulse is considered to study the plastic behavior of Cu.

https://doi.org/10.1017/S026303460700064X Published online by Cambridge University Press

3.2. Lead Target

In this case the target is a lead cylinder with length equal to 7 mm and radius equal to 5 mm. Again, one face of the target is irradiated with a uranium beam having particle energy of 400 MeV/u. The beam pulse consists of two bunches, each having a FWHM of 80 ns, and the total pulse duration is 500 ns. The beam focal spot size (FWHM of the Gaussian power distribution in transverse direction) is assumed to be 1.0 mm. The following two values for the beam intensity are used.

3.2.1. Case III

$N = 2.5 \times 10^7$ ions per pulse is considered to study the elastic properties of Pb.

3.2.2. Case IV

$N = 5.5 \times 10^7$ ions per pulse is considered to study the plastic behavior of Pb.

3.3. Tantalum Target

In this set of experiments, tantalum cylinders, each with length and radius = 5 mm are used. The target is facially irradiated with a uranium beam having particle energy of 400 MeV/u. The beam focal spot size (FWHM of the Gaussian power distribution in transverse direction) is assumed to be 0.5 mm. The following three values for beam intensity, N are used.

3.3.1. Case V

$N = 5.0 \times 10^7$ ions per pulse is considered to study the elastic properties of Ta. The beam pulse consists of two bunches, each having a FWHM of 80 ns and the total pulse duration is 500 ns.

3.3.2. Case VI

$N = 1.5 \times 10^8$ ions per pulse is considered to study the plastic behavior of Ta. The beam pulse consists of two bunches, each having a FWHM of 80 ns and the total pulse duration is 500 ns.

3.3.3. Case VII

$N = 4 \times 10^9$ ions per pulse is considered to study the material rupture. In this case, the beam pulse consists of four bunches, each having a FWHM of 80 ns and the total pulse duration is 1 μs.

3.4. Tungsten Target

For tungsten, we considered four different cases using cylindrical target, each with length and radius equal to 5 mm as described below. The targets are facially irradiated with uranium beam having particle energy of 400 MeV/u.

3.4.1. Case VIII

$N = 5 \times 10^7$ ions per pulse that is composed of two bunches with the total pulse length equal to 500 ns. The beam spot size (FWHM) equal to 0.5 mm and this experiment will be performed to study elastic properties of W.

3.4.2. Case IX

$N = 1.5 \times 10^8$ ions per pulse that again consists of two bunches with the total pulse length equal to 500 ns. The beam spot size (FWHM) equal to 0.5 mm and this experiment will be carried out to study plasticity in W.

3.4.3. Case X

$N = 1.25 \times 10^8$ ions per pulse that consists of a single Gaussian bunch that is 250 ns long (FWHM = 80 ns). The beam spot size (FWHM) equal to 1.0 mm.

3.4.4. Case XI

$N = 5.0 \times 10^8$ ions per pulse that consists of four Gaussian bunches each 250 ns long (FWHM = 80 ns) so that the total pulse length is 1 μs. The beam spot size (FWHM) = 1.0 mm. A comparison between simulation results obtained in case X and case XI will show the effect of beam time structure on the target response.

3.5. Solid Graphite Target

The following two cases have been considered for graphite target. These experiments will generate physical conditions that will be somewhat similar to those simulated in Tahir *et al.* (2005*c*).

3.5.1. Case XII

$N = 2.0 \times 10^9$ ions per pulse that again consists of four Gaussian bunches equally distributed so that the total pulse length is 1 μs. The standard deviation, σ of the spatial power distribution (Gaussian) = 0.5 mm. The target length as well as the radius is 5 mm so the target length is less than the ion range.

3.5.2. Case XIII

$N = 4.0 \times 10^9$ ions per pulse whereas the rest of the beam parameters are the same as in case XII. The spatial power distribution is a Gaussian with a standard deviation, $\sigma = 2.0$ mm. The target length is 15 mm while the radius is 5 mm. In this case, the target length is larger than the ion range so that the Bragg peak will lie inside the target.

4. THREE-DIMENSIONAL COMPUTER CODE

The 3D computer code that has been used to do these calculations is based on a modified particle in cell (PIC) method.

https://doi.org/10.1017/S026303460700064X Published online by Cambridge University Press

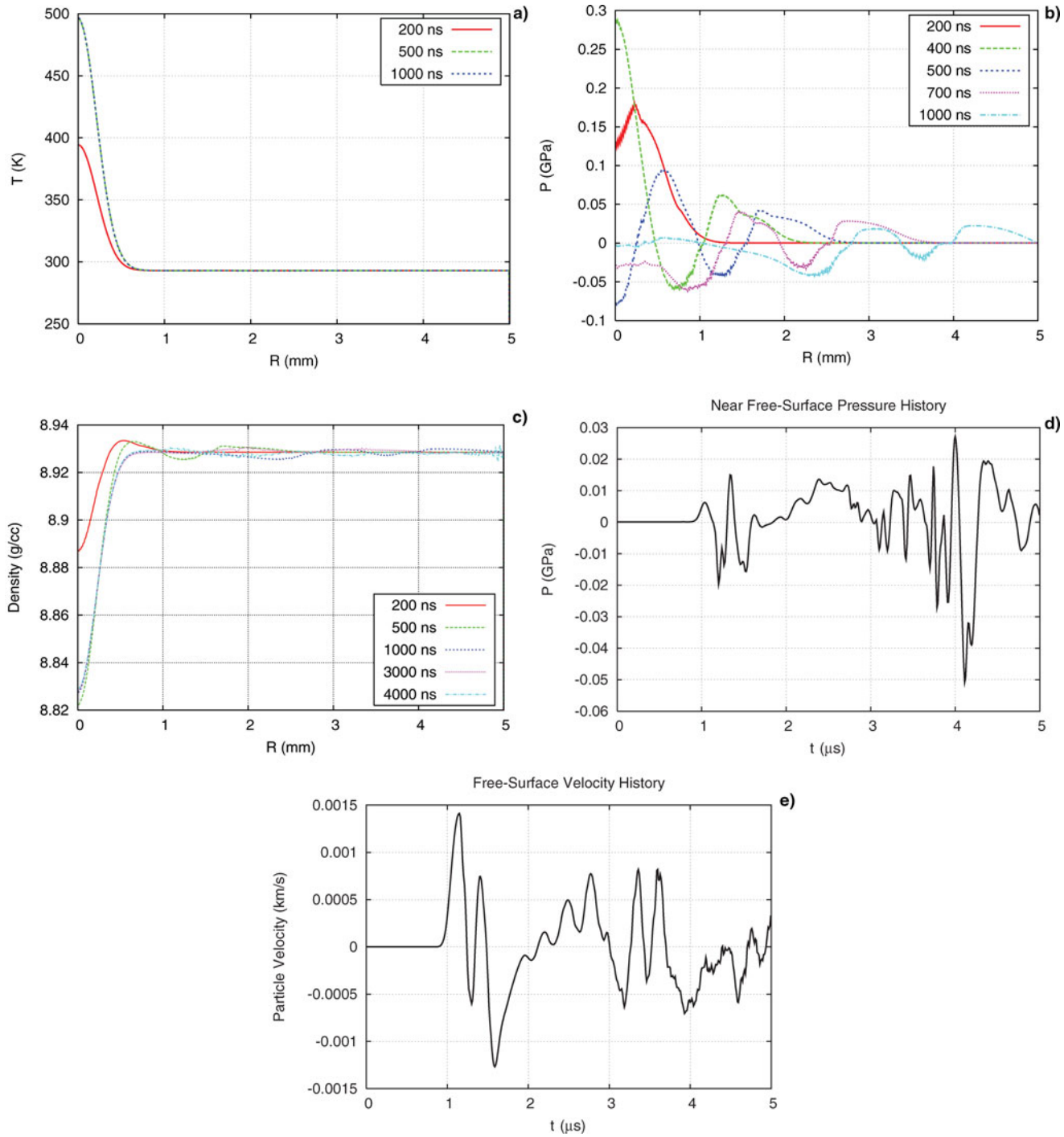

Fig. 1. (Color online) Cu cylinder, $L = 7$ mm, $r = 5$ mm, $N = 5 \times 10^7$ uranium ions, two successive Gaussian bunches (FWHM = 80 ns), pulse duration = 500 ns, spot size (FWHM) = 0.5 mm: (**a**) Temperature versus radius (at $L = 3.5$ mm) at different times; (**b**) Pressure versus radius (at $L = 3.5$ mm) at different times; (**c**) Density versus radius (at $L = 3.5$ mm) at different times; (**d**) Pressure at the surface (at $L = 3.5$ mm) as a function of time; (**e**) Surface velocity (at $L = 3.5$ mm) as a function of time.

The energy loss from the projectile particles is handled employing a full 3D particle tracking scheme while the target physical conditions are treated using a sophisticated semi-empirical equation-of-state (EOS) model (Bushman *et al.*, 1993). Elastic effects are treated using a model of ideal elasticity that means Hook's law complemented with yield criteria. To describe material flow in elastic regime, Prandtl-Reuse equation is used:

$$s_{ij}^{n+1} = s_{ij}^{n+2} + 2 \cdot G\left(e_{ij} - \frac{1}{3}\delta_{ij} Tr\hat{V}\right),$$

https://doi.org/10.1017/S026303460700064X Published online by Cambridge University Press

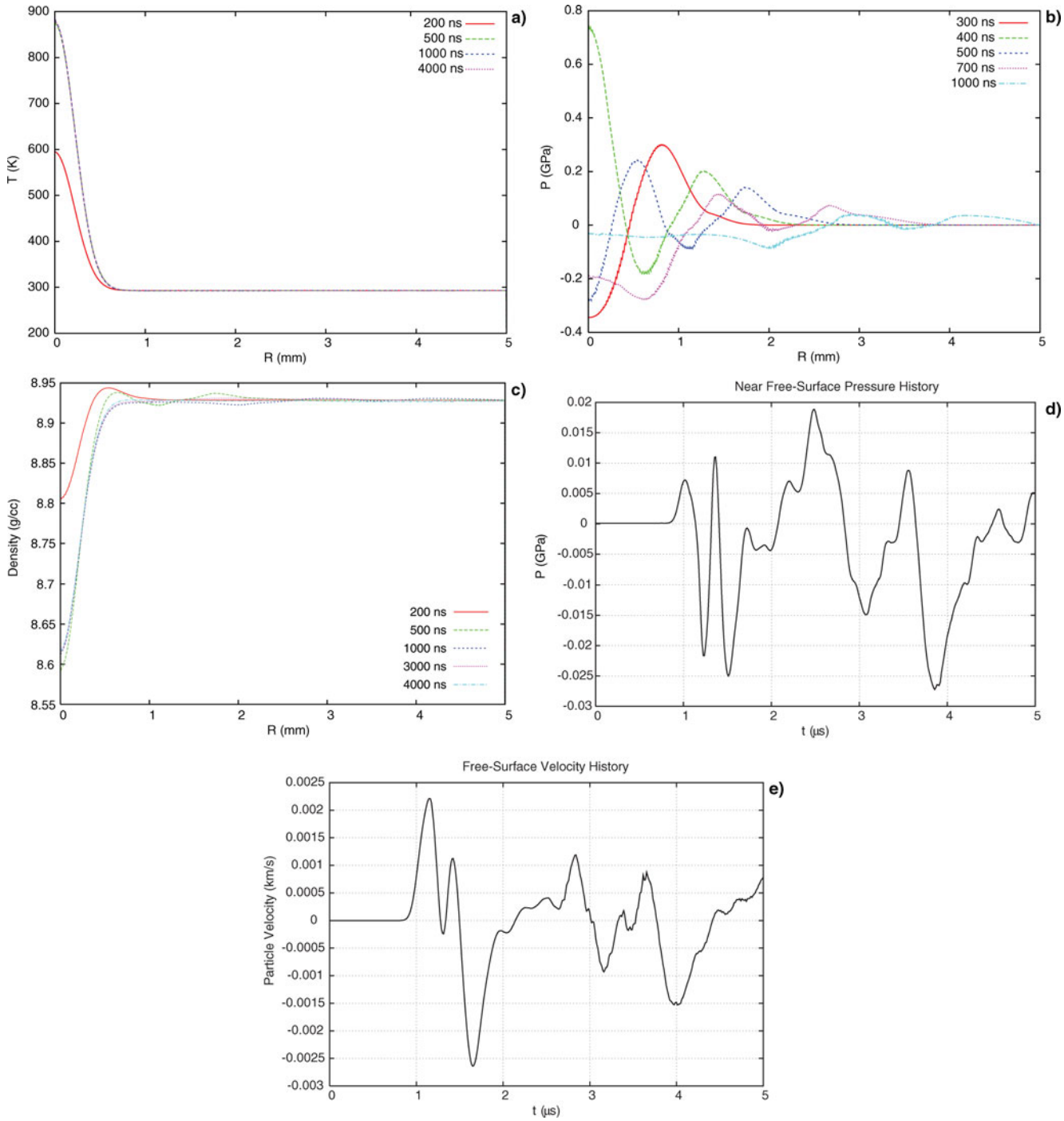

Fig. 2. (Color online) Cu cylinder, $L = 7$ mm, $r = 5$ mm, $N = 1.5 \times 10^8$ uranium ions, two successive Gaussian bunches (FWHM = 80 ns), pulse duration = 500 ns, spot size (FWHM) = 0.5 mm: (**a**) Temperature versus radius (at $L = 3.5$ mm) at different times; (**b**) Pressure versus radius (at $L = 3.5$ mm) at different times; (**c**) Density versus radius (at $L = 3.5$ mm) at different times; (**d**) Pressure at the surface (at $L = 3.5$ mm) as a function of time; (**e**) Surface velocity (at $L = 3.5$ mm) as a function of time.

where $e_{ij} = 1/2\ (\partial\ \bar{v}_i/\partial\ x_j + \partial\ \bar{v}_j/\partial\ x_i)$ is components of strain tensor $\hat{V}$, δ_{ij} is Kronecker's delta and G is the shear Modulus. To describe plastic regime of material deformation, von Misses yield criterion with Wilkins normalizing procedure is used in the following form:

$$s_{ij} = \begin{cases} s_{ij}, & \mathrm{J} < \frac{2}{3} Y_0 \\ s_{ij} \cdot \sqrt{\frac{2}{3} Y_0^2 \sqrt{J}}, & \mathrm{J} > \frac{2}{3} Y_0 \end{cases}$$

https://doi.org/10.1017/S026303460700064X Published online by Cambridge University Press

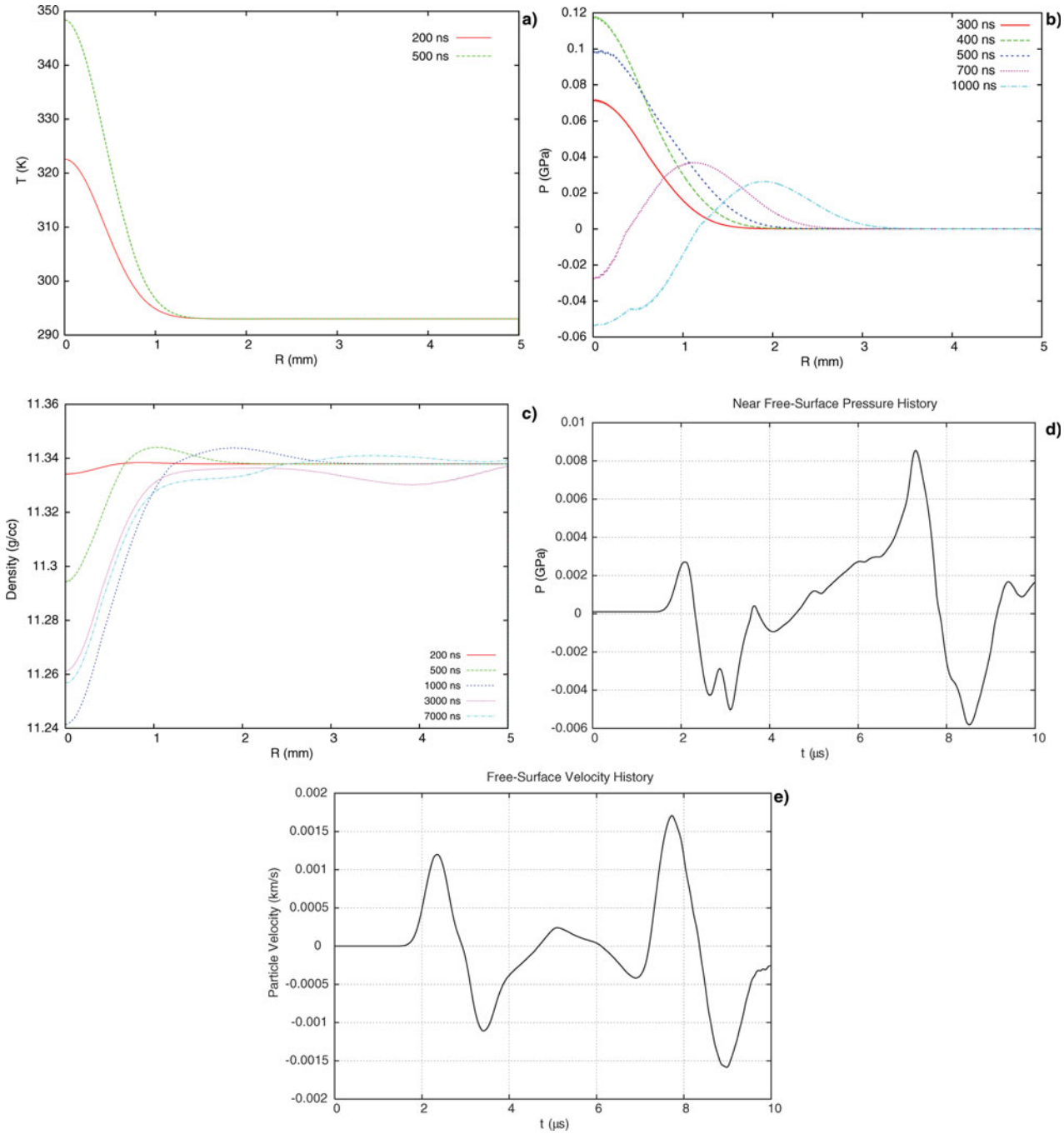

Fig. 3. (Color online) Pb cylinder, $L = 7$ mm, $r = 5$ mm, $N = 2.5 \times 10^7$ uranium ions, two successive Gaussian bunches (FWHM = 80 ns), pulse duration = 500 ns, spot size (FWHM) = 1.0 mm: (**a**) Temperature versus radius (at $L = 3.5$ mm) at different times; (**b**) Pressure versus radius (at $L = 3.5$ mm) at different times; (**c**) Density versus radius (at $L = 3.5$ mm) at different times; (**d**) Pressure at the surface (at $L = 3.5$ mm) as a function of time; (**e**) Surface velocity (at $L = 3.5$ mm) as a function of time.

where $J = \Sigma_{i=x}^{z} \Sigma_{j=x}^{z} s_{ij}^2$, Y_0 is yield strength and s_{ij} is the deviatoric part of the stress tensor.

5. NUMERICAL SIMULATION RESULTS

In this section we present numerical simulations results for the cases noted in Section 3. Assuming the azimuthal symmetry, we have done two-dimensional (2D) simulations using the 3D code. The results are given below.

5.1. Copper Target

5.1.1. Case I

The target is longer than the range of the projectile particles and the Bragg peak lies inside the target. The

https://doi.org/10.1017/S026303460700064X Published online by Cambridge University Press

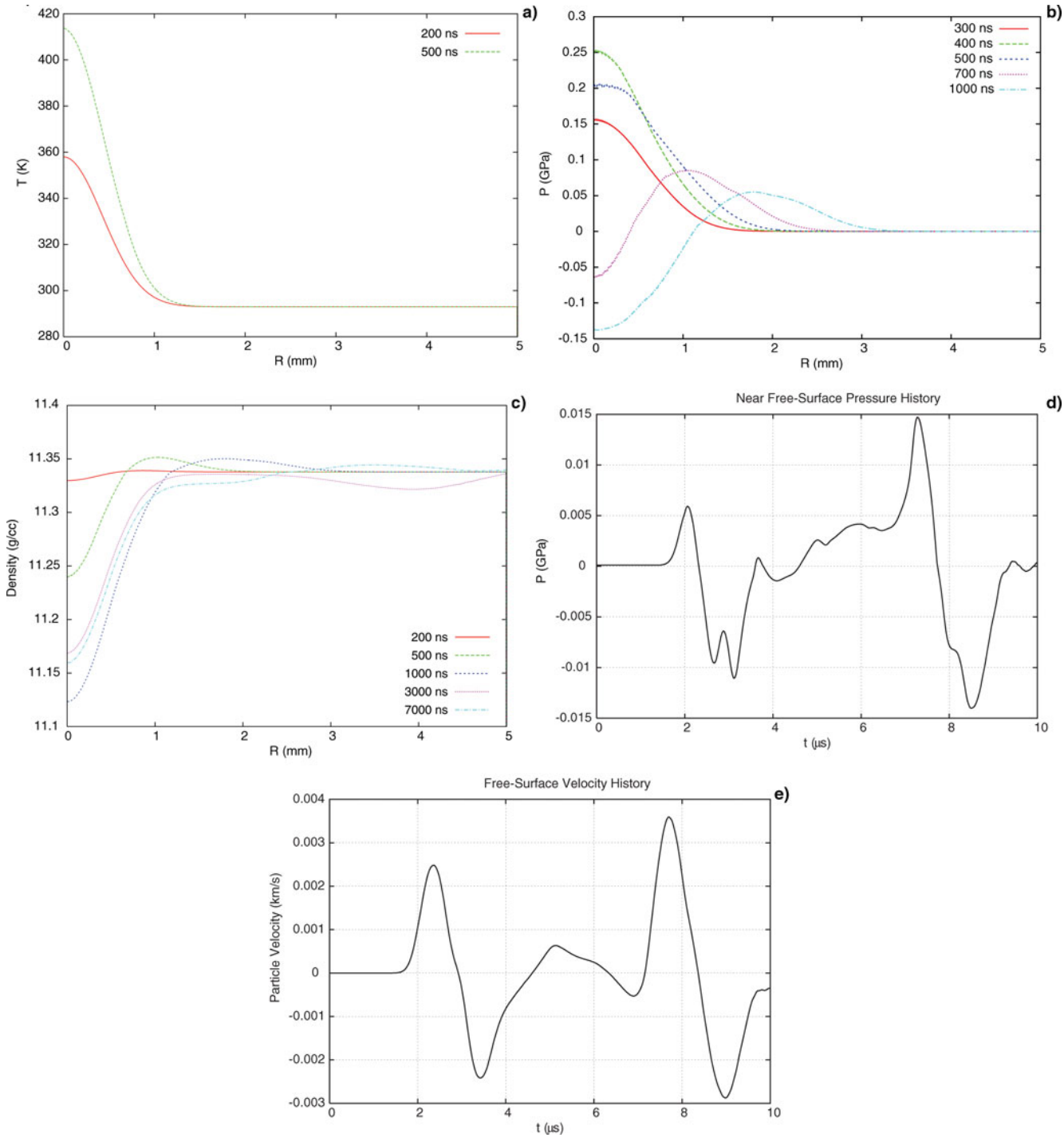

Fig. 4. (Color online) Pb cylinder, $L = 7$ mm, $r = 5$ mm, $N = 5.5 \times 10^7$ uranium ions, two successive Gaussian bunches (FWHM = 80 ns), pulse duration = 500 ns, spot size (FWHM) = 1.0 mm: (**a**) Temperature versus radius (at $L = 3.5$ mm) at different times; (**b**) Pressure versus radius (at $L = 3.5$ mm) at different times; (**c**) Density versus radius (at $L = 3.5$ mm) at different times; (**d**) Pressure at the surface (at $L = 3.5$ mm) as a function of time; (**e**) Surface velocity (at $L = 3.5$ mm) as a function of time.

maximum specific energy deposition in this case is on the order 0.24 kJ/g. In Figure 1a, we plot the temperature versus radius at L = 3.5 mm. It is seen that as a result of energy deposition by the first bunch, the temperature increases to a peak value of about 400 K at the center (profile at $t = 200$ ns), and due to energy deposition by the second bunch, the temperature increases to about 500 K. Figure 1b shows the corresponding pressure profiles that show propagation of pressure waves in the target. Figure 1c shows that the density does not undergo any significant

https://doi.org/10.1017/S026303460700064X Published online by Cambridge University Press

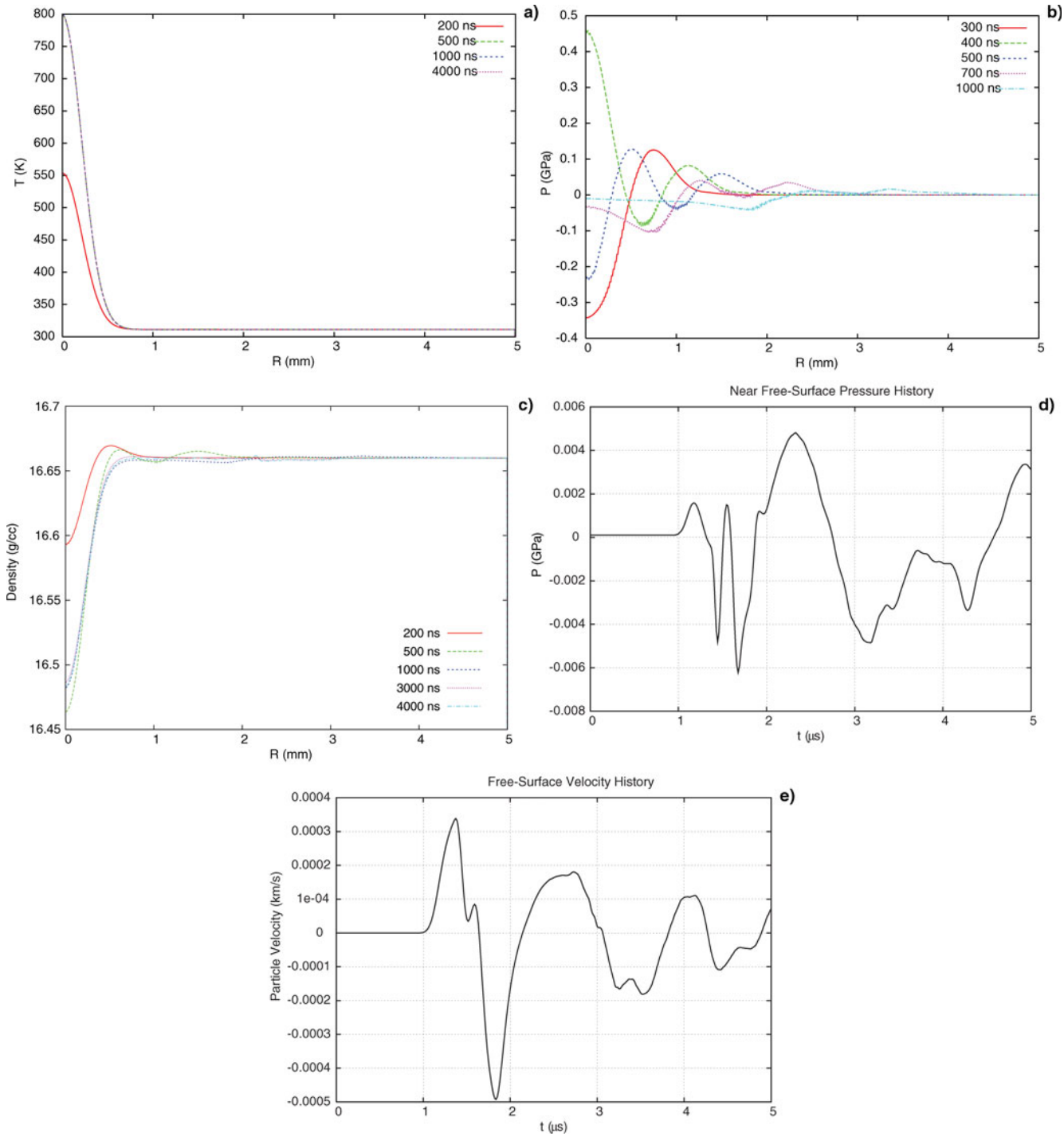

Fig. 5. (Color online) Ta cylinder, $L = 5$ mm, $r = 5$ mm, $N = 5.0 \times 10^7$ uranium ions, two successive Gaussian bunches (FWHM = 80 ns), pulse duration = 500 ns, spot size (FWHM) = 0.5 mm: (**a**) Temperature versus radius (at $L = 2.5$ mm) at different times; (**b**) Pressure versus radius (at $L = 2.5$ mm) at different times; (**c**) Density versus radius (at $L = 2.5$ mm) at different times; (**d**) Pressure at the surface (at $L = 2.5$ mm) as a function of time; (**e**) Surface velocity (at $L = 2.5$ mm) as a function of time.

change in this case. In Figure 1d, we plot the surface pressure at point $L = 3.5$ mm as a function of time. The surface velocity as a function of time is given in Figure 1e. It is seen that the maximum surface velocity is about 1.5 m/s. The oscillations damp out with time because the material is in elastic regime. It is to be noted that the main diagnostic tool in these experiments, will be a laser Doppler vibrometer (LDV) that will be used to measure the instantaneous velocity, and displacement of the vibrating target surface from the Doppler shift in the frequency of back-scattered laser light (Mazumder *et al.*, 1970), and a direct comparison of the experimental measurements with Figure 1e will be very useful.

https://doi.org/10.1017/S026303460700064X Published online by Cambridge University Press

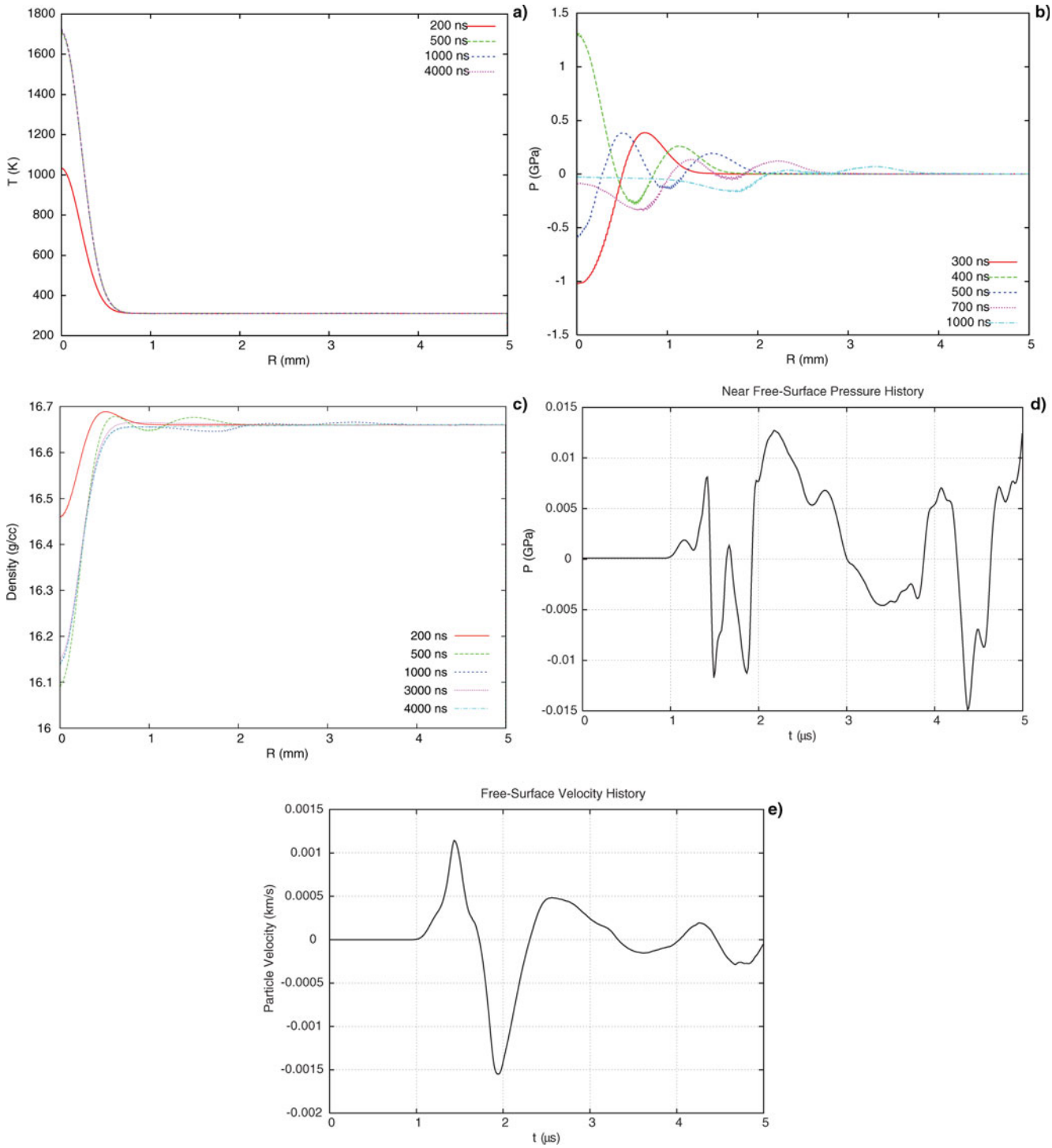

Fig. 6. (Color online) Ta cylinder, $L = 5$ mm, $r = 5$ mm, $N = 1.5 \times 10^8$ uranium ions, two successive Gaussian bunches (FWHM = 80 ns), pulse duration = 500 ns, spot size (FWHM) = 0.5 mm: (**a**) Temperature versus radius (at $L = 2.5$ mm) at different times; (**b**) Pressure versus radius (at $L = 2.5$ mm) at different times; (**c**) Density versus radius (at $L = 2.5$ mm) at different times; (**d**) Pressure at the surface (at $L = 2.5$ mm) as a function of time; (**e**) Surface velocity (at $L = 2.5$ mm) as a function of time.

5.1.2. Case II

In this case, the beam intensity is higher than that used in Case I, we achieve a higher specific energy deposition of 0.7 kJ/g. This leads to a higher temperature (see Fig. 2a) as well as a higher pressure (see Fig. 2b). The density in this case also does not show any significant change. The surface pressure and surface velocity versus time are plotted in Figures 2d and 2e, respectively, which again show an oscillatory behavior.

https://doi.org/10.1017/S026303460700064X Published online by Cambridge University Press

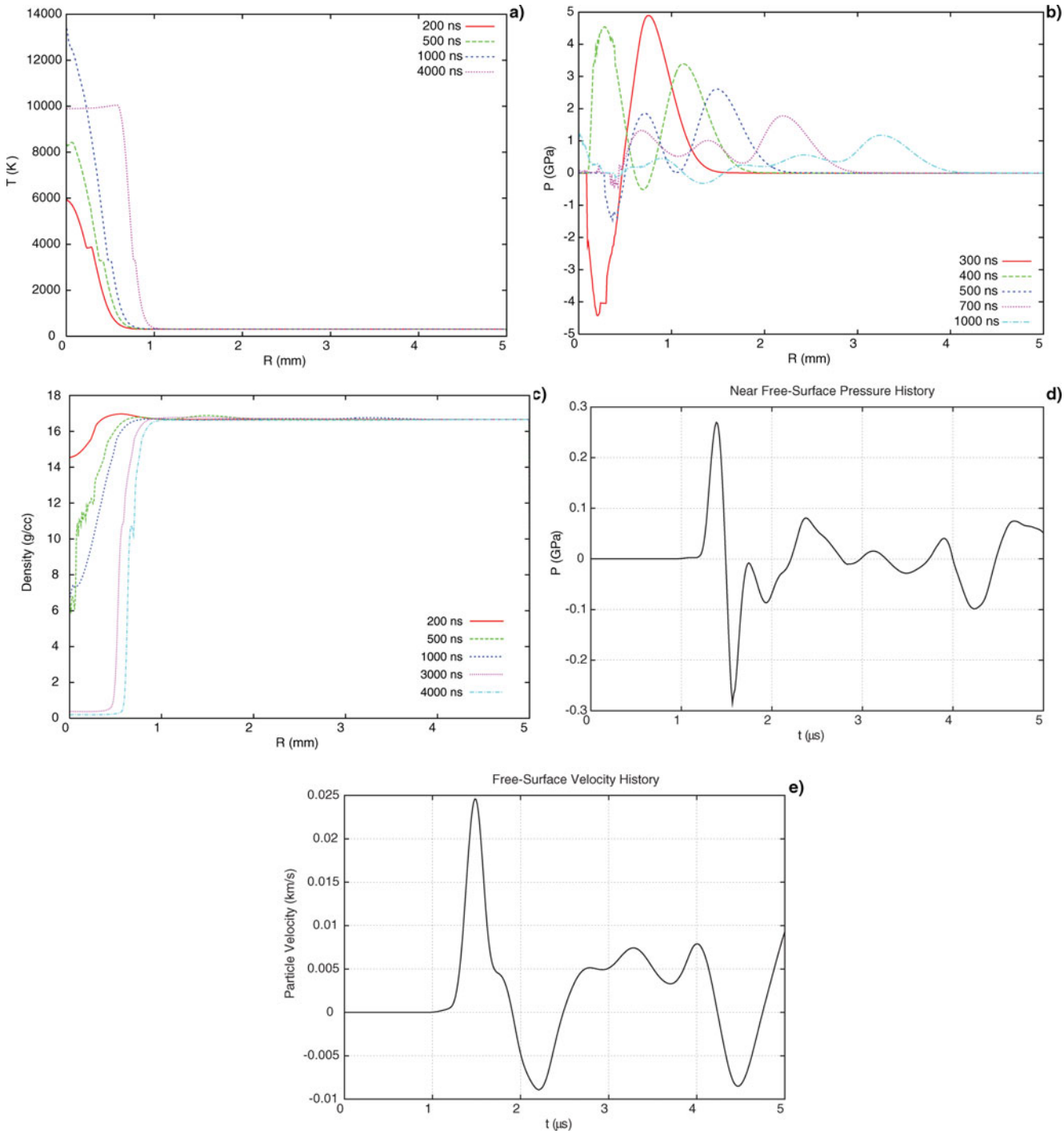

Fig. 7. (Color online) Ta cylinder, $L = 5$ mm, $r = 5$ mm, $N = 4.0 \times 10^9$ uranium ions, four successive Gaussian bunches (FWHM = 80 ns), pulse duration = 1000 ns, spot size (FWHM) = 0.5 mm: (**a**) Temperature versus radius (at $L = 2.5$ mm) at different times; (**b**) Pressure versus radius (at $L = 2.5$ mm) at different times; (**c**) Density versus radius (at $L = 2.5$ mm) at different times; (**d**) Pressure at the surface (at $L = 2.5$ mm) as a function of time; (**e**) Surface velocity (at $L = 2.5$ mm) as a function of time.

5.2. Lead Target

5.2.1. Case III

The Bragg peak lies inside the target and the maximum specific energy in this case is 0.176 kJ/g. The temperature, pressure, and density profiles for this case are plotted in Figures 3a, 3b, and 3c, respectively. A maximum temperature of about 350 K is achieved whereas the maximum pressure is on the order of 0.12 GPa. The density practically remains unchanged. The surface pressure and the surface velocity at point $L = 3.5$ mm as a function of time are plotted in Figures 3d and 3e, respectively.

https://doi.org/10.1017/S026303460700064X Published online by Cambridge University Press

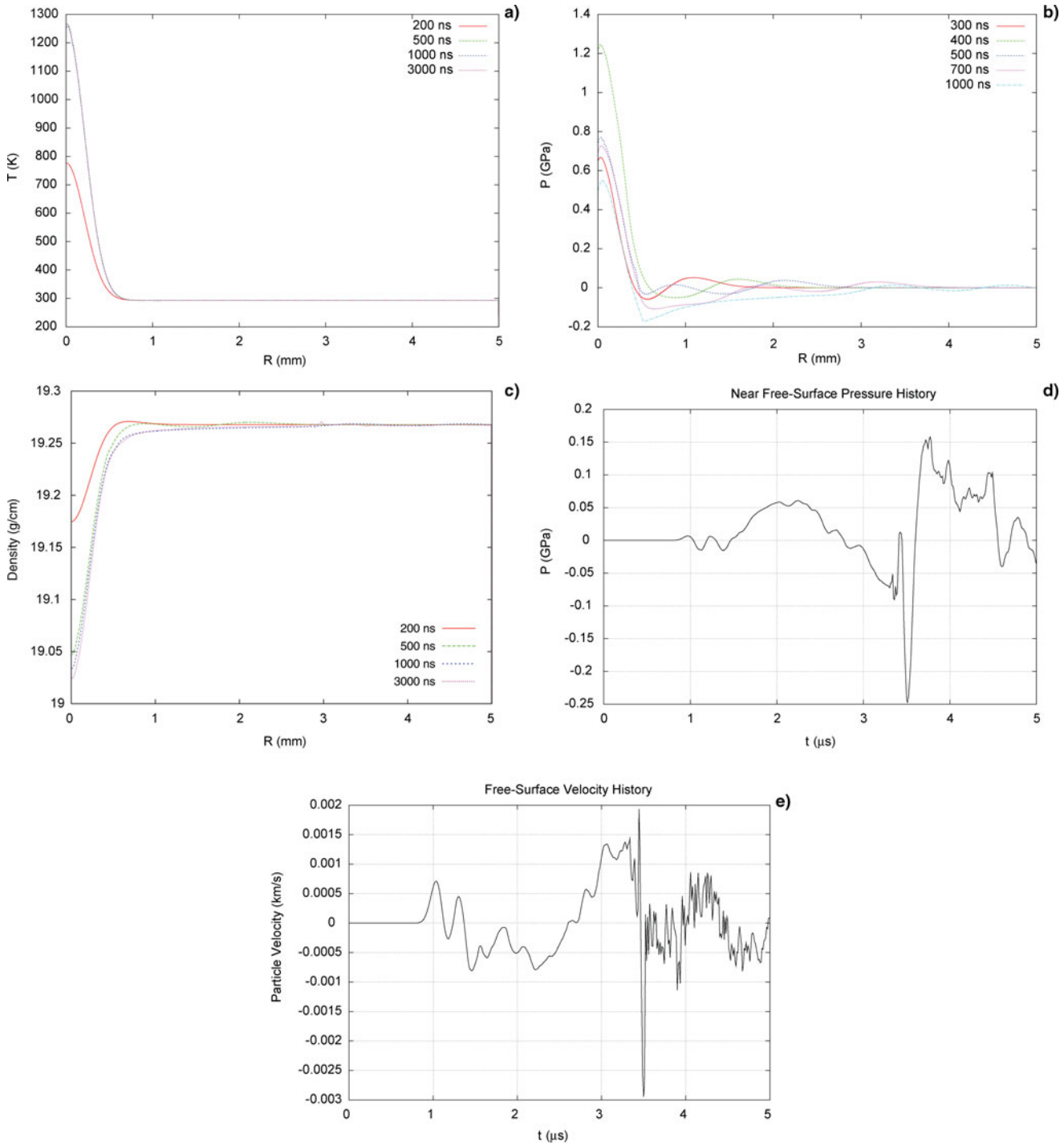

Fig. 8. (Color online) W cylinder, $L = 5$ mm, $r = 5$ mm, $N = 5.0 \times 10^7$ uranium ions, two successive Gaussian bunches (FWHM = 80 ns), pulse duration = 500 ns, spot size (FWHM) = 0.5 mm: (**a**) Temperature versus radius (at $L = 2.5$ mm) at different times; (**b**) Pressure versus radius (at $L = 2.5$ mm) at different times; (**c**) Density versus radius (at $L = 2.5$ mm) at different times; (**d**) Pressure at the surface (at $L = 2.5$ mm) as a function of time; (**e**) Surface velocity (at $L = 2.5$ mm) as a function of time.

5.2.2. Case IV

In this case, a specific energy deposition of about 0.48 kJ/g is achieved, and the results are plotted in Figures 4a–4e. It seems that the maximum temperature is about 410 K, maximum pressure is on the order of 0.25 GPa, whereas the density remains practically unchanged. Figure 4e shows that the surface velocity has a value of 3 m/s.

https://doi.org/10.1017/S026303460700064X Published online by Cambridge University Press

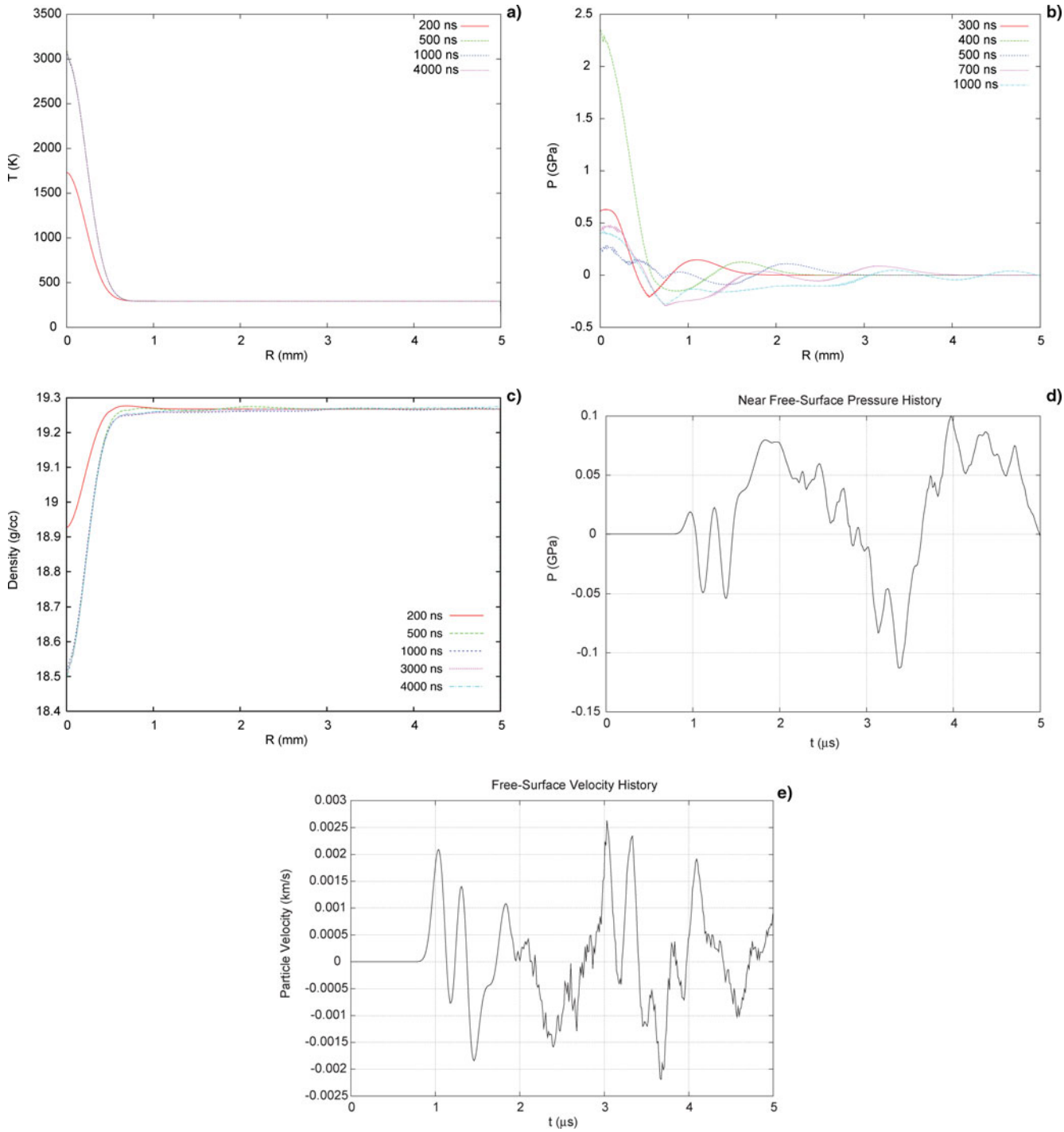

Fig. 9. (Color online) W cylinder, $L = 5$ mm, $r = 5$ mm, $N = 1.5 \times 10^8$ uranium ions, two successive Gaussian bunches (FWHM = 80 ns), pulse duration = 500 ns, spot size (FWHM) = 0.5 mm: (**a**) Temperature versus radius (at $L = 2.5$ mm) at different times; (**b**) Pressure versus radius (at $L = 2.5$ mm) at different times; (**c**) Density versus radius (at $L = 2.5$ mm) at different times; (**d**) Pressure at the surface (at $L = 2.5$ mm) as a function of time; (**e**) Surface velocity (at $L = 2.5$ mm) as a function of time.

5.3. Tantalum Target

5.3.1. Case V

Figure 5a shows a maximum temperature of 800 K while Figure 5b indicates a maximum pressure of 0.45 GPa while Figure 5c does not show any significant change in the density. The surface pressure (Fig. 5d) and the surface velocity (Fig. 5e) show an oscillatory behavior and the maximum surface velocity is about 3 m/s.

https://doi.org/10.1017/S026303460700064X Published online by Cambridge University Press

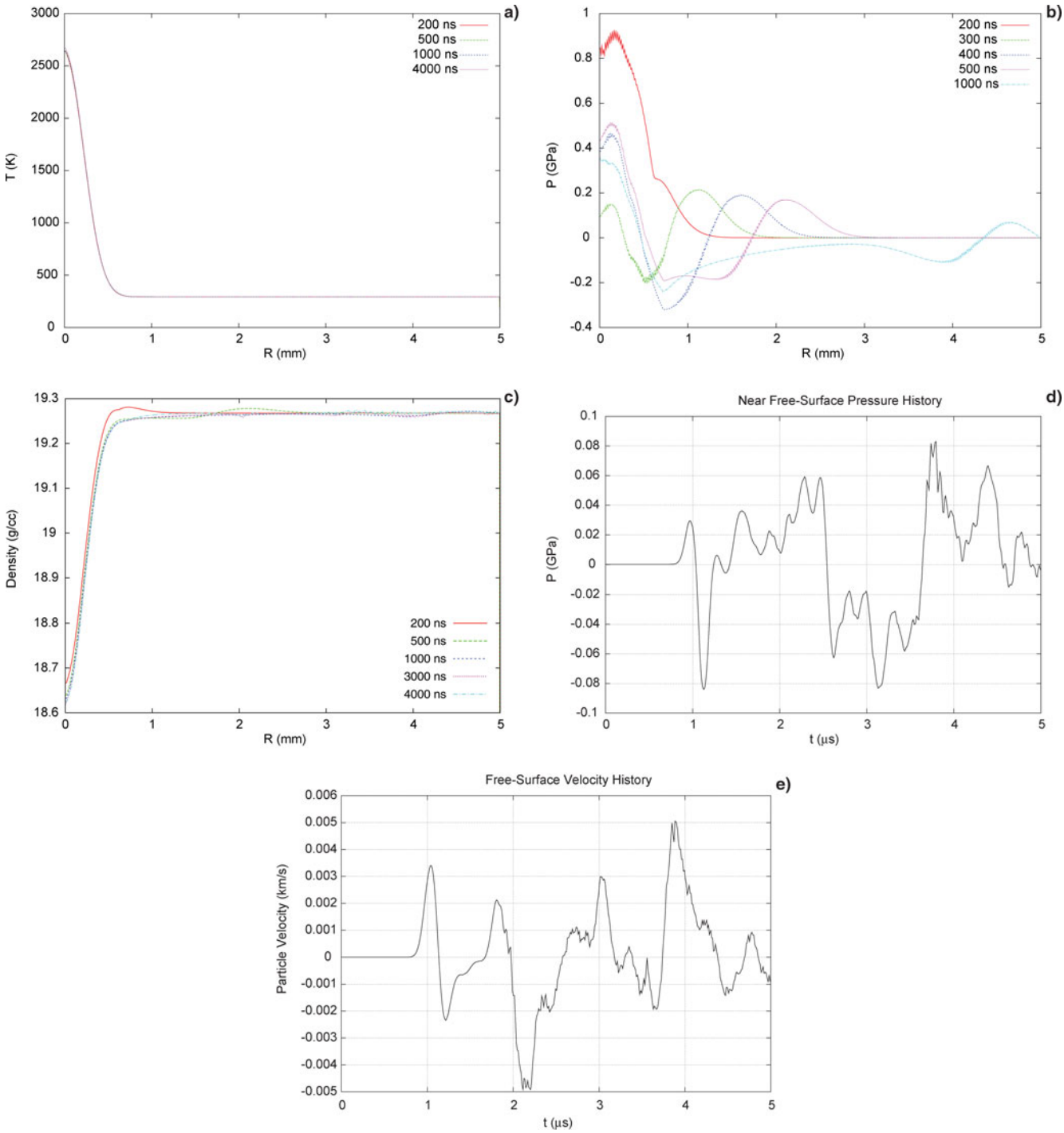

Fig. 10. (Color online) W cylinder, $L = 5$ mm, $r = 5$ mm, $N = 1.25 \times 10^8$ uranium ions, single Gaussian bunches (FWHM = 80 ns), pulse duration = 250 ns, spot size (FWHM) = 0.5 mm: (**a**) Temperature versus radius (at $L = 2.5$ mm) at different times; (**b**) Pressure versus radius (at $L = 2.5$ mm) at different times; (**c**) Density versus radius (at $L = 2.5$ mm) at different times; (**d**) Pressure at the surface (at $L = 2.5$ mm) as a function of time; (**e**) Surface velocity (at $L = 2.5$ mm) as a function of time.

5.3.2. Case VI

In this case, we achieve a maximum temperature of 1700 K (Fig. 6a) and a maximum pressure of about 1 GPa (Fig. 6b) while Figure 6c does not show any significant change in the density. Surface pressure versus time (Fig. 6d) and surface velocity versus time (Fig. 6e) show an oscillatory behavior.

5.3.3. Case VII

In this case, the maximum beam intensity is used and a maximum temperature of 14000 K (Fig. 7a) is achieved that leads to evaporation of the target at the center, maximum pressure of 5 GPa is achieved (Fig.7b) and time structure of four bunches is clearly seen. Moreover, the density at the

https://doi.org/10.1017/S026303460700064X Published online by Cambridge University Press

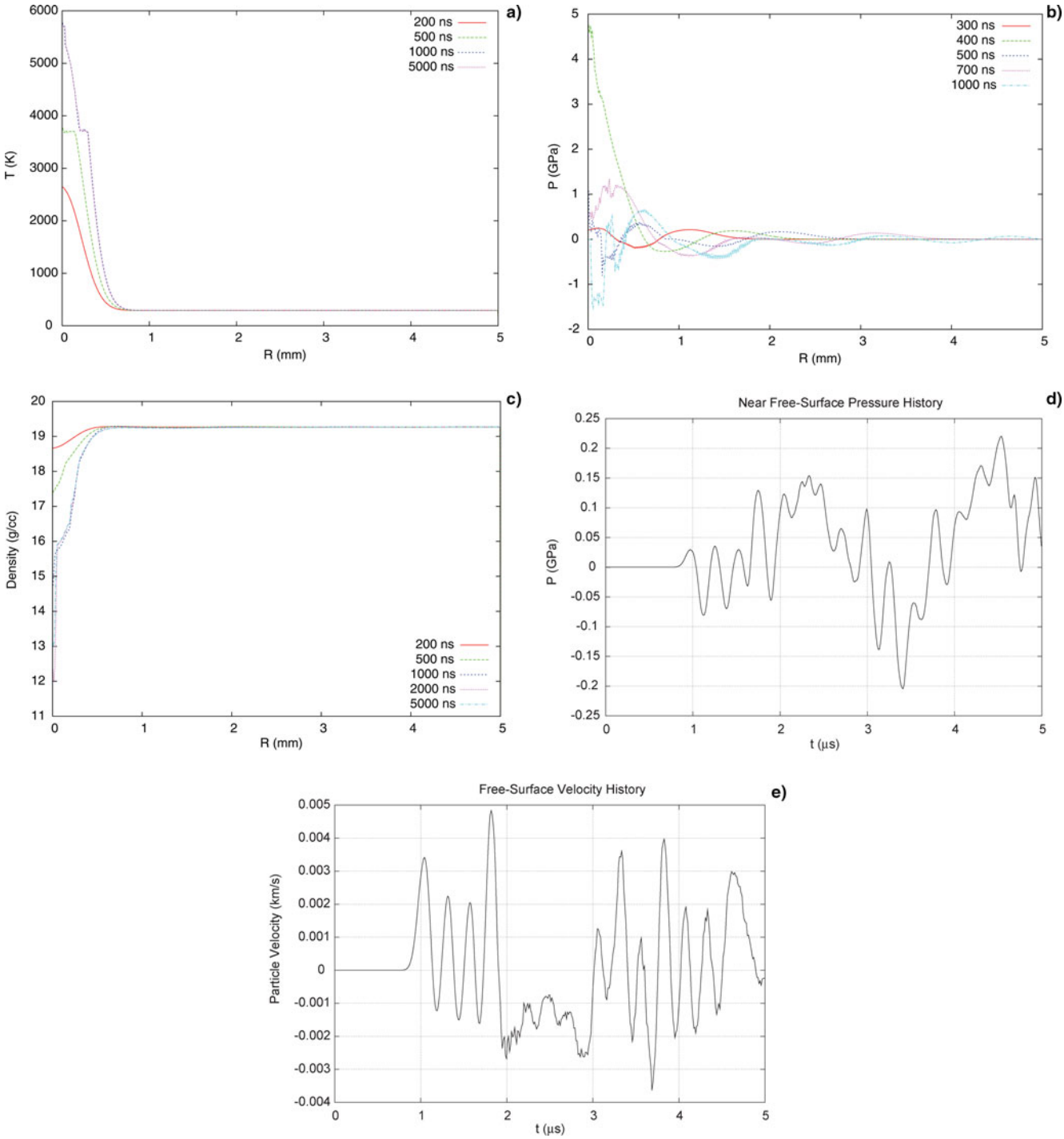

Fig. 11. (Color online) W cylinder, $L = 5$ mm, $r = 5$ mm, $N = 50 \times 10^8$ uranium ions, four successive Gaussian bunches (FWHM = 80 ns), pulse duration = 1000 ns, spot size (FWHM) = 0.5 mm: (**a**) Temperature versus radius (at $L = 2.5$ mm) at different times; (**b**) Pressure versus radius (at $L = 2.5$ mm) at different times; (**c**) Density versus radius (at L = 2.5 mm) at different times; (**d**) Pressure at the surface (at $L = 2.5$ mm) as a function of time; (**e**) Surface velocity (at $L = 2.5$ mm) as a function of time.

target center is substantially reduced due to the outgoing radial shock wave. It is seen from Figures 7d and 7e that the surface pressure and the surface velocity show little oscillations that implies that the material is permanently damaged.

5.4. Tungsten Target

5.4.1. Case VIII

Figures 8a and 8b, respectively, show that a maximum temperature of 1250 K and a maximum pressure of 1.2 GPa

https://doi.org/10.1017/S026303460700064X Published online by Cambridge University Press

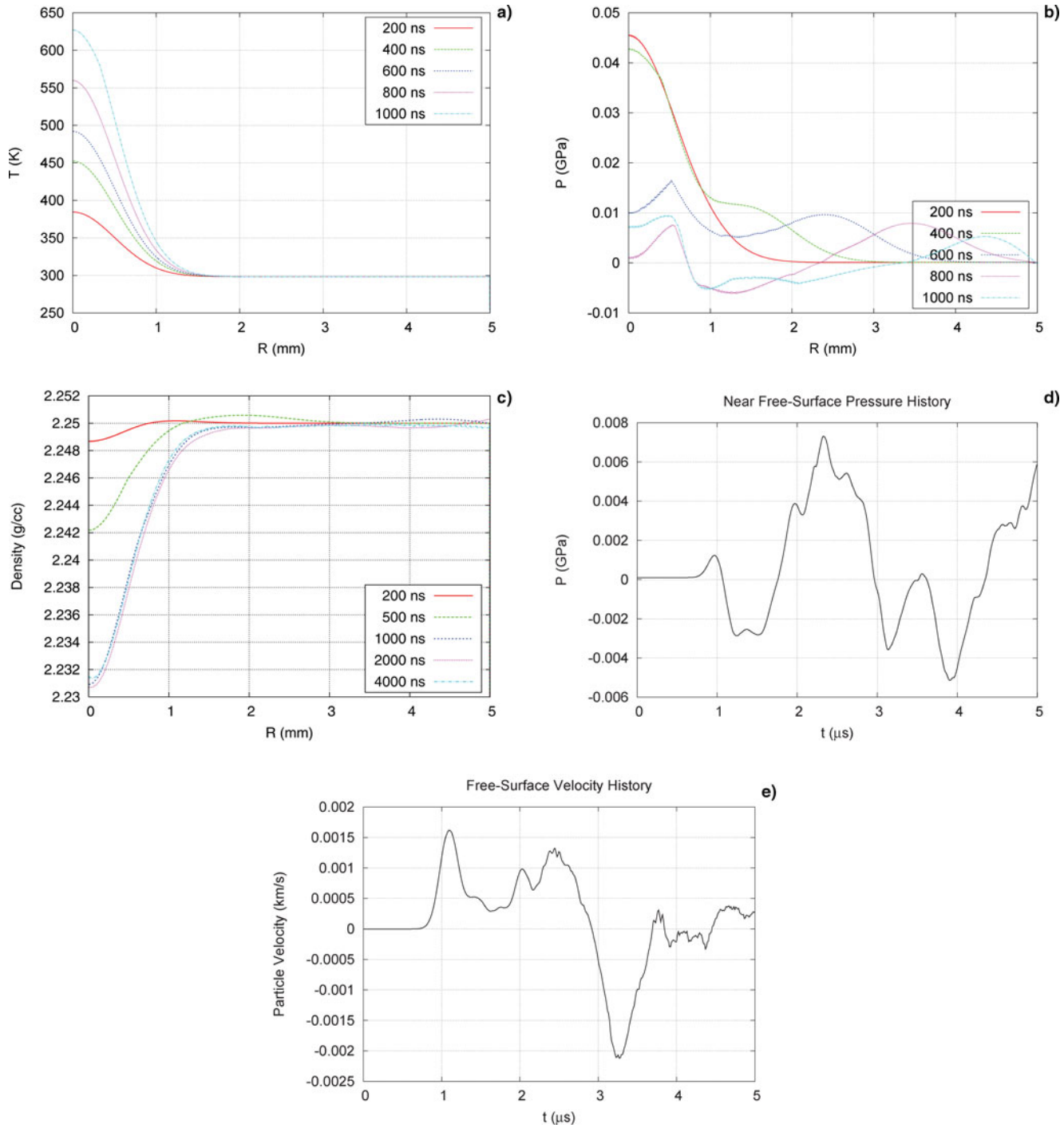

Fig. 12. (Color online) C cylinder, $L = 5$ mm, $r = 5$ mm, $N = 2.0 \times 10^9$ uranium ions, five successive Gaussian bunches (FWHM = 80 ns), pulse duration = 1000 ns, spot size (standard deviation, σ) = 0.5 mm: (**a**) Temperature versus radius (at $L = 2.5$ mm) at different times; (**b**) Pressure versus radius (at $L = 2.5$ mm) at different times; (**c**) Density versus radius (at $L = 2.5$ mm) at different times; (**d**) Pressure at the surface (at $L = 2.5$ mm) as a function of time; (**e**) Surface velocity (at $L = 2.5$ mm) as a function of time.

are achieved in this case, while Figure 8c shows no significant change in density. Figures 8d and 8e, respectively, show the surface pressure and the surface velocity as a function of time. It is seen that the surface velocity is very small.

5.4.2. Case IX

The results are plotted in Figures 9a–9e, respectively. It is seen from the Figures that a maximum temperature of 3000 K and a maximum pressure of about 2 GPa is achieved in this

https://doi.org/10.1017/S026303460700064X Published online by Cambridge University Press

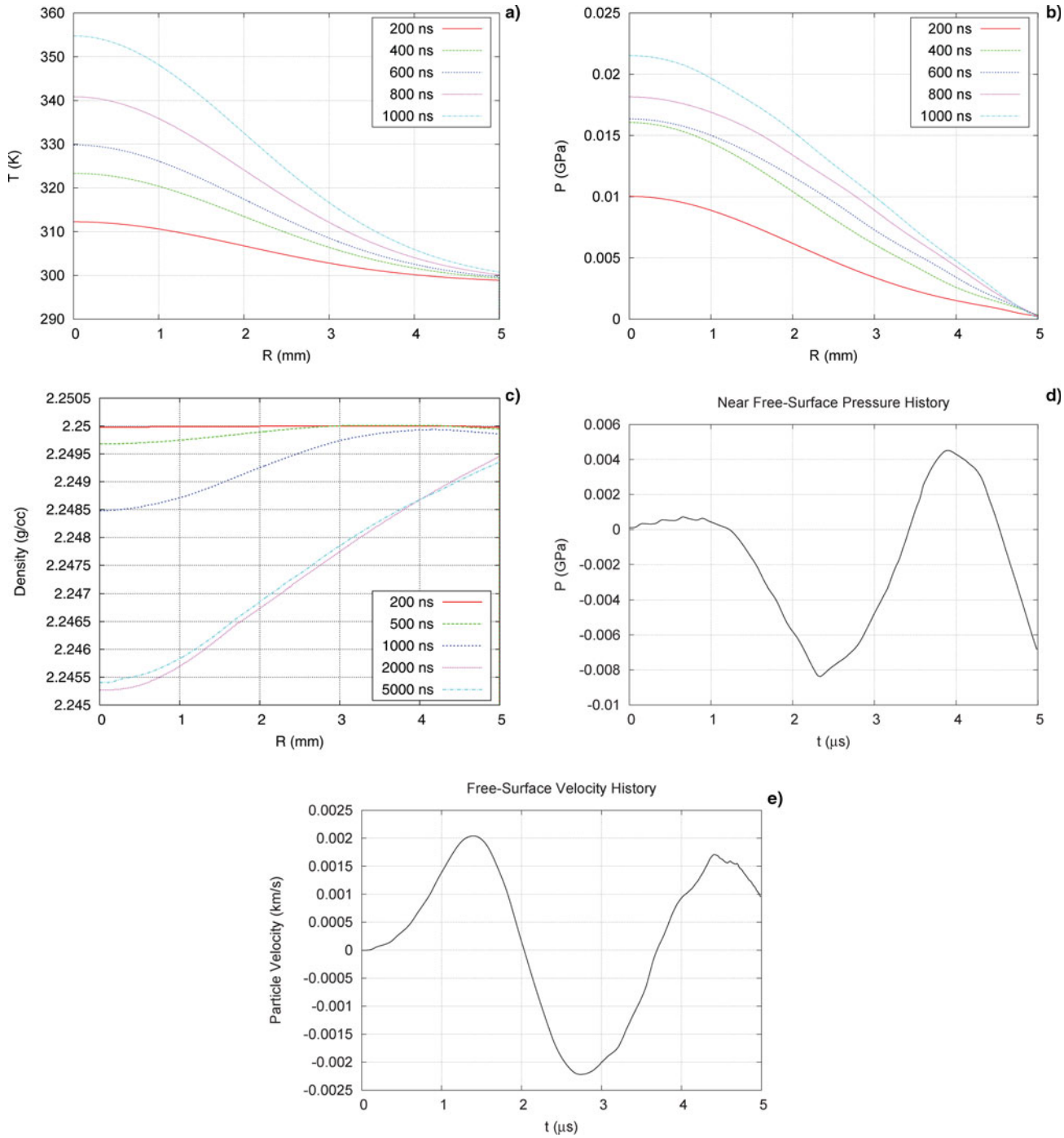

Fig. 13. (Color online) C cylinder, $L = 15$ mm, $r = 5$ mm, $N = 4.0 \times 10^9$ uranium ions, five successive Gaussian bunches (FWHM = 80 ns), pulse duration = 1000 ns, spot size (standard deviation, σ) = 2.0 mm: (**a**) Temperature versus radius (at $L = 2.5$ mm) at different times; (**b**) Pressure versus radius (at $L = 2.5$ mm) at different times; (**c**) Density versus radius (at $L = 2.5$ mm) at different times; (**d**) Pressure at the surface (at $L = 2.5$ mm) as a function of time; (**e**) Surface velocity (at $L = 2.5$ mm) as a function of time.

case. The surface pressure and the surface velocity show a nice oscillatory behavior.

5.4.3. *Case X*

In this case, a single bunch is used, one sees a simple temperature profile with a maximum value above 2000 K (Fig. 10a) whereas the pressure profiles in Figure 10b shows a typical picture of radially outgoing pressure waves that are reflected at the boundary. Figure 10c again shows that the density remains almost unchanged.

5.4.4. *Case XI*

The results are plotted in Figures 11a–11e. It is seen that the target center is heated to a temperature of about 6000 K

https://doi.org/10.1017/S026303460700064X Published online by Cambridge University Press

(Fig. 11a) while a maximum pressure of 5 GPa is achieved. The material at the target center is evaporated and the density is substantially reduced due to outgoing compression wave. Figures 11d and 11e) show a nice oscillatory structure. The effect on the time structure of the four bunches is also visible in profiles of different variables.

5.5. Carbon Target

For carbon we considered two cases and the results are presented below.

5.5.1. Case XII

It is seen from Figure 12a that the maximum temperature at the end of the pulse (after the fourth bunch), is on the order of 600 K, whereas Figure 12b shows that a maximum pressure of 0.045 GPa is achieved at $t = 200$ ns (at the end of the first bunch). This is because, as the pressure increases, a pressure wave is launched radially outwards that decreases the pressure at the target center, before the pressure can increase due to energy deposition by the second bunch. Since thermal conductivity is not very effective at such low temperatures and due to the high density, the temperature continues to increase as more bunches deposit their energy. Figure 12c shows that the density remains almost unchanged whereas one sees nice oscillatory behavior of surface pressure and surface velocity from Figures 12d and 12e, respectively.

5.5.2. Case XIII

In this case, although the intensity is two times higher than that in Case XII, the focal spot is four times larger that leads to a lower deposition. The results are plotted in Figures 13a–13e.

6. CONCLUSIONS

In this paper, we presented numerical simulations for heating of target of different materials including lead, tantalum, Wolfram, copper, and solid graphite using an uranium ion beam with a particle energy of 400 MeV/u. Different time structures have been considered for the ion pulse that include a single bunch, two successive bunches and four bunches. Different beam spot sizes and different beam intensities have been considered. The purpose of this work is to simulate propagation of thermally induced stress waves in such targets. The parameters used in this theoretical study match those of experiments that will be carried out in the near future at the GSI Plasma Physics experimental area. A direct comparison between the experimental and simulation results will be useful in interpretation of the experiments.

AKNOWLEGDMENTS

The authors wish to thank H. Richter and A. Kelic for providing the beam and target parameters to do these simulations. This work was financially supported by the BMBF, Germany and RFBR grant No.06–02–04011–NNIOa, Russia.

REFERENCES

Bushman, A.V., Kanel, G.I., Ni, A.L. & Fortov, V.E. (1993). Thermophysics and dynamics of intense pulsed loadings. London, UK: Taylor and Francis.

Fabich, A. & Lettery, J. (2003). Experimental observation of protoninduced shocks and magneto-fluid-dynamics in liquid metal. *Nucl. Instrum. Meth Phys. Res. A* **503**, 336.

Geissel, H., Weick, H., Münzenberg, G., Chichkine, V., Yavor, M., Aumann, T., Behr, K.H., Böhmer, A., Brünle, A., Burkahrd, K., Benlliure, J., Cortina-Gil, D., Chulkov, L., Dael, A., Ducret, J.-E., Emling, H., Franczak, B., Friese, J., Gastineau, B., Gerl, J., Gernhäuser, R., Hellström, M., Johnson, B., Kojouharova, J., Kulessa, R., Kindler, B., Kurz, N., Lommel, B., Mittig, W., Moritz, G., Mühle, Nolen, J.A., Nyman, G., Rousell-Chomaz, P., Scheindenberger, C., Schmidt, K.-H., Schrieder, G., Sherrill, B.M., Simon, H., Sümmerer, K., Tahir, N.A., Vysotsky, V., Wollnik, H. & Zeller, A.F. (2003). The Super-FRS project at GSI. *Nucl. Instrum. Meth Phys. Res. B* **204**, 71.

Heidenreich, G. (2002). Carbon and beryllium targets at PSI. *High Inten. High Bright. Hadron Beams* **642**, 124.

Henning, W.F. (2004). The future GSI facility. *Nucl. Instrum. Meth. Phys. Res. B*. **214**, 155.

Hoffmann, D.H.H., Blazevic, A., Ni, P., Rosmej, O., Roth, M., Tahir, N.A., Tauschwitz, A., Udrea, S., Varentsov, D., Weyrich, K. & Maron, Y. (2005). Present and future perspectives of high energy density physics with intense ions and laser beams. *Laser Part. Beams* **23**, 47.

Lopez Cela, J.J., Piriz, A.R., Serena Moreno, M. & Tahir, N.A. (2006). Numerical simulations of Rayleigh–Taylor instability in elastic solids. *Laser Part. Beams* **24**, 427.

Mazumder, M. K. (1970). Laser doppler velocity measurement without directional ambiguity by using frequency shifted incident beams. *Appl. Phys. Lett.* **16**, 462.

Nolen, J.A., Reed, C.B., Hassanein, A., Novick, V.J., Plotkin, P., Specht, J.R., Morrissey, D.J., Ottarson, J.H. & Sherrill, B.M. (2003). An adjustable thickness Li/Be target for fragmentation of 4-kW heavy ion beams. *Nucl. Instrum. Meth Phys. Res. B* **204**, 293.

Piriz, A.R., Portugues, R.F., Tahir, N.A., Hofmann, D.H.H. (2002). Implosion of multilayered cylindrical targets driven by intense heavy ion beams. *Phys. Rev. E* **66**, 056403.

Piriz, A.R., Temporal, M., Lopez Cela, J.J., Tahir, N.A. & Hoffmann, D.H.H. (2003). Symmetry analysis of cylindrical implosions driven by high-frequency rotating ion beams. *Plasma Phys. Contr. Fusion* **45**, 1733.

Piriz, A.R., Temporal, M., Lopez Cela, J.J., Tahir, N.A. & Hoffmann, D.H.H. (2005). Rayleigh-Taylor instability in elastic solids. *Phys. Rev. E* **72**, 056313.

Piriz, A.R., Lopez Cela, J.J., Serena Moreno, M., Tahir, N.A. & Hoffmann, D.H.H. (2006). Thin plate effects in the Rayleigh-Taylor instability of elastic solids. *Laser Part. Beams* **24**, 275.

Piriz, A.R., Tahir, N.A., Lopez Cela, J.J., Cortazar, O.D., Serna Moreno, M.C., Temporal, M. & Hoffmann, D.H.H. (2007).

https://doi.org/10.1017/S026303460700064X Published online by Cambridge University Press

Analytic models for the design of the LAPLAS target. *Contrib. Plasma Phys*. **47**, 213.

Piriz, A.R., Lopez Cela, J.J., Serna Moreno, M.C., Cortazar, O.D., Tahir, N.A. & Hoffmann, D.H.H. (2007). A new approach to Rayleigh–Taylor instability: Applications to accelerated elastic solids. *Nucl. Instrum. Meth Phys. Res. A* **577**, 250.

Ray, A., Srivastava, M.K., Kodayya, G. & Menon, S.V.G. (2006). Improved equation of state of metals in the liquid-vapor region. *Laser Part. Beams* **24**, 437.

Tahir, N.A., Hoffmann, D.H.H., Kozyreva, A., Shutov, A., Maruhn, J.A., Neuner, U., Tauschwitz, A., Spiller, P. & Bock, R. (2000*a*). Shock compression of condensed matter using intense beams of energetic heavy ions. *Phys. Rev. E.* **61**, 1975.

Tahir, N.A., Hoffmann, D.H.H., Kozyreva, A., Shutov, A., Maruhn, J.A., Neuner, U., Tauschwitz, A., Spiller, P. & Bock, R. (2000*b*). Equation-of-state properties of high-energy-density matter using intense heavy ion beams with an annular focal spot. *Phys. Rev. E* **62**,1224.

Tahir, N.A., Kozyreva, Spiller, P., Hoffmann, D.H.H. & Shutov, A. (2001*a*). Necessity of bunch compression for heavy-ion-induced hydrodynamics and studies of beam fragmentation in solid targets at a proposed synchrotron facility. *Phys. Rev. E*. **63**, 036407.

Tahir, N.A., Hoffmann, D.H.H., Kozyreva, A., Tauschwitz, A., Shutov, A., Maruhn, J.A., Spiller, P., Nuener, U., Jacoby, J., Roth, M., Bock, R., Juranek, H. & Redmer, R. (2001*b*). Metallization of hydrogen using heavy-ion-beam implosion of multi-layered targets. *Phys. Rev. E* **63**, 016402.

Tahir, N.A., Juranek, H., Shutov, A., Redmer, R., Piriz, A.R., Temporal, M., Varentsov, D., Udrea, S., Hoffmann, D.H.H., Deutsch, C., Lomonosov, I. & Fortov, V. E. (2003*b*). Influence of the equation of state on the compression and heating of hydrogen. *Phys. Rev. B*. **67**, 184101.

Tahir, N.A., Winkler, M., Kojouharova, J., Rousell-Chomaz, P., Chichkine, V., Geissel, H., Hoffmann, D.H.H., Kindler, B., Landre-Pellemoine, F., Lommel, B., Mittig, W., Münzenberg, G., Shutov, A., Weick, H. & Yavor, M. (2003*a*). High-power production targets for the Super-FRS using a fast extraction scheme. *Nucl. Instrum. Meth. Phys. Res. B* **204**, 282.

Tahir, N.A., Adonin, A., Deutsch, C., Fortov, V.E., Grandjouan, N., Geil, B., Gryaznov, V., Hoffmann, D.H.H., Kulish, M., Lomonosov, I.V., Mintsev, V., Ni, P., Nikolaev, D., Piriz, A.R., Shilkin, N., Spiller, P., Shuto, A., Temporal, M., Ternovoi, V., Udrea, S.Varentsov, D. (2005*b*). Studies of heavy ion-induced highenergy density states in matter at the GSI Darmstadt SIS-18 and future FAIR facility. *Nucl. Instrum. Meth. Phys. Res. A* **544**, 16.

Tahir, N.A., Deutsch, C., Fortov, V.E., Gryaznov, V., Hoffmann, D.H.H., Kulish, M., Lomonosov, I.V., Mintsev, V., Ni, P., Nikolaev, D., Piriz, A.R.,Shilkin, N., Spiller, P., Shutov, A., Temporal, M., Ternovoi, V., Udrea, S. & Varentsov, D. (2005*c*). Proposal for the study of thermophysical properties of high-energy-density matter using current and future heavy ion accelerator facilities at GSI Darmstadt. *Phys. Rev. Lett*. **95**, 035001.

Tahir, N.A., Weick, H., Iwase, H., Geissel, H., Hoffmann, D.H.H., Kindler, B., Lommel, B., Radon, T., Münzenberg, G. & Sümmerer, K. (2005*d*). Calculations of high-power production target and beamdump for the GSI future Super-FRS for a fast extraction scheme at the FAIR facility. *J. Phys. D: Appl. Phys*. **38**, 1828.

Tahir, N.A., Goddard, B., Kain, V., Schmidt, R., Shutov, A., Lomonosov, I.V., Piriz, A.R., Temporal, M., Hoffmann, D.H.H. & Fortov, V.E. (2005*e*). Impact of 7-Tev/c large hadron collider proton beam on a copper target. *J. Appl. Phys*. **97**, 083532.

Tahir, N.A., Kain, V., Schmidt, R., Shutov, A., Lomonosov, I.V., Gryaznov, V., Piriz, A.R., Temporal, M., Hoffmann, D.H.H. & Fortov, V.E. (2005*d*). The CERN large hadron collider as a tool to study high-energy-density physics. *Phys. Rev. Lett*. **94**, 135004.

Tahir, N.A., Spiller, P., Udrea, S., Cortazar, O.D., Deutsch, C., Fortov, V.E., Gryaznov, V., Hoffmann, D.H.H., Lomonosov, I.V., Ni, P., Piriz, A.R., Shutov, A., Temporal, M. & Varentsov, D. (2006). Studies of equation-of-state properties of high-energy density matter using intense heavy ion beams at the future FAIR facility: The HEDgeHOB collaboration. *Nucl. Instrum. Meth. Phys. Res. B* **245**, 85.

Tahir, N.A., Spiller, P., Shutov, A., Lomonosov, I.V., Gryaznov, V., Piriz, A.R., Wouchuk, G., Deutsch, C., Fortov, V.E., Hoffmann, D.H.H. & Schmidt, R. (2007). HEDgeHOB: High-energy density matter generated by heavy ion beams at the future facility for antiprotons and ion research. *Nucl. Instrum. Meth. Phys. Res. A* **577**, 238.

Tahir, N.A., Piriz, A.R., Shutov, A., Lomonosov, I.V., Gryaznov, V., Wouchuk, G., Deutsch, C., Spiller, P., Fortov, V.E., Hoffmann, D.H.H. & Schmidt, R. (2007). Survey of theoretical work for the proposed HEDgeHOB collaboration: HIHEX and LAPLAS. *Contrib. Plasma Phys*. **47**, 223.

Tahir, N.A., Kim, V., Grigoriev, D.A., Piriz, A.R., Weick, H., Geissel, H. & Hoffmann, D.H.H. (2007). High energy density physics problems related to liquid jet lithium target for Super-FRS fast extraction scheme. *Laser Part. Beams* **25**, 295.

Temporal, M., Lopez-Cela, J.J., Piriz, A.R., Grandjouan, N., Tahir, N.A. & Hoffmann, D.H.H. (2003). Numerical analysis of a multilayered cylindrical target compression driven by a rotating intense heavy ion beam. *Laser Part. Beams* **21**, 609.

Temporal, M., Lopez-Cela, J.J., Piriz, A.R., Grandjouan, N., Tahir, N.A. & Hoffmann, D.H.H. (2005). Compression of a cylindrical hydrogen sample driven by an intense co-axial heavy ion beam. *Laser Part. Beams* **23**, 137.

https://doi.org/10.1017/S026303460700064X Published online by Cambridge University Press